ELSEVIER

Chemical Engineering Journal 137 (2008) 205–213

Chemical Engineering Journal

www.elsevier.com/locate/cej

On the effect of wax content on paraffin wax deposition in a batch oscillatory baffled tube apparatus

Lukman Ismail, Robin E. Westacott, Xiongwei Ni *

Centre for Oscillatory Baffled Reactor Applications (COBRA), Chemical Engineering, School of Engineering and Physical Sciences, Heriot-Watt University, Edinburgh EH14 4AS, United Kingdom

Received 21 August 2006; received in revised form 9 March 2007; accepted 14 April 2007

Abstract

Deposition of paraffin wax is one of the major problems facing in the petroleum industries with the main implication being wax blockage in oil and gas pipelines especially for offshore production. The objectives of this work are to investigate the effect of applying oscillatory motion on wax deposition in an oscillatory baffled tube apparatus, a relatively new mixing technology that offers more uniform mixing and solid suspension than traditional devices; and are to understand the mechanism and kinetics of the wax crystallisation in accordance to the Avrami theory. The wax deposition was determined gravimetrically. The results indicate that the oscillatory motion has two opposite effects on the percentage of wax deposition: at low concentration of wax in solution, the presence of oscillation significantly reduces the wax deposition, e.g. 40–60% without the presence of any solvent or wax inhibitor; and completely prevents 100% wax gelation from occurring – the beneficial effect; at higher wax contents, however, the introduction of oscillatory motion not only promotes wax deposition, but also accelerates the crystal growth to achieve 100% wax deposition – the detrimental effect.

Keywords: Paraffin; Wax deposition; Oscillatory motion; Baffles; Supersaturation; Bulk crystallisation; Avrami theory

1. Introduction

Extraction of crude oil from offshore reservoirs usually endures serious problems such as the obstruction of pipelines. Oil enters the pipeline at 60–70 °C and because the ocean water is much colder (4 °C in deep waters); the oil is cooled causing heavy hydrocarbons to precipitate out as the oil flows through the pipeline. The precipitated wax deposits on the tube inner wall, forming a solid layer that narrows the flow passage and eventually reduces the flow rates [1]. Traditional methods of management, prevention and remediation have been established over many years which involve mechanical means such as pigging, thermal treatment such as circulation of warm liquid, and chemical treatment such as addition of solvent and/or dispersant [2].

Much of the research conducted in the area of wax deposition has been centred around predicting and modelling of wax deposition, see for examples, the prediction of flocculation from petroleum fluids [3]; the prediction of the viscosity of waxy oils [4,5]; the improved thermodynamic model for wax precipitation [6]; the prediction of the phase behaviour of petroleum fluids [7]; the prediction of wax deposition for flow assurance [8]; and the new thermodynamic model validated with wax disappearance temperature [44].

Laboratory investigations on wax deposition have been carried out such as using a cold finger set-up [9,10]; using flow loops set-up [11]; in multiphase flow [12]; in a glass inner layer pipe [13]; in cooled heat exchanger tubes [14]; determining wax deposition using heat transfer method [15] and solvent migration in a paraffin deposit [16]. Examples of studies in mitigation of wax deposition can be found, e.g. using high velocity flow [2]; using the combined shear and flow improvers [17]; inductive heating of pipelines [18] application of glass inner layer [13] addition of chemical wax inhibitor [19,20] using Nd–Fe–B magnets [21,45] and use of exothermic chemical reactions [22]. In this work, we introduce a relatively new device, the oscillatory baffled tube apparatus (OBTA), which is completely different from these aforementioned.

OBTA is a mixing technology and offers more uniform mixing and particle suspension than traditional reactors. The fluid

* Corresponding author. Tel.: +44 1314513781; fax: +44 1314513129.
E-mail address: x.ni@hw.ac.uk (X. Ni).

1385-8947/$ – see front matter © 2007 Elsevier B.V. All rights reserved.
doi:10.1016/j.cej.2007.04.018

Nomenclature

D_c	column diameter (m)
f	oscillation frequency (Hz)
K	growth rate (min^{-1})
n	the Avrami exponent
Re_o	oscillatory Reynolds number ($=2\pi f x_o \rho_L D_c/\mu$)
St	Strouhal number ($=D_c/4\pi x_o$)
V_t	volume or volume fraction of crystallisation
x_o	centre-to-peak amplitude of oscillation (m)
X	degree of crystallisation

Greek letters

ρ_L	fluid density ($kg\,m^{-3}$)
δ_0	initial wax in liquid (%)
δ_∞	the maximum or asymptotic deposition (%)
δ_r	relative deposition (%)
δ_t	the total deposition at time t (%)
μ	fluid viscosity ($kg\,m^{-1}\,s^{-1}$)

dynamic conditions in an OBTA are governed by two dimensionless groups, namely, the oscillatory Reynolds number (Re_o) and the Strouhal number (St), defined as

$$Re_o = \frac{2\pi f x_o \rho_L D_c}{\mu} \quad (1)$$

$$St = \frac{D_c}{4\pi x_o} \quad (2)$$

where ρ_L is the fluid density ($kg\,m^{-3}$), μ the fluid viscosity ($kg\,m^{-1}\,s^{-1}$), D_c the column diameter (m), x_o the oscillation amplitude (m) and f is the oscillation frequency (Hz). The oscillatory Reynolds number describes the intensity of oscillation applied to the system, using the peak velocity of oscillation as the characteristic velocity and the column diameter as the characteristic dimension. The Strouhal number is inversely proportional to the amplitude of oscillation and represents the ratio of column diameter to stroke length, a measure of the effective eddy propagation. The product of $2\pi f x_o$ is the maximum oscillatory velocity (m/s). This study has been prompted by the idea that the enhanced mixing in OBTA could lead to increase suspension of wax particles (with liquid) thereby reducing either the total deposition or the deposition rate. In this paper, an experimental investigation into wax deposition in the OBTA is reported, focusing on the effects of the paraffin wax content with changing oscillation frequencies and amplitudes on the percentage of wax deposition.

2. Mechanism

The mechanism of wax deposition in oil pipeline is largely via nucleation and crystallisation processes where oil is entrapped between crystals leading to gel formation and can be treated as bulk crystallisation [11]. Consequently, the Avrami phase transition equation is the well-known principle in describing such crystallisation kinetics. The original derivations by Avrami [23] have been simplified by Evans [24] and put into polymer context by Meares [25] and Hay [26]. The basic principle can be illustrated by imagining raindrops falling in a puddle. The raindrops produce expanding circles of waves which intersect and cover the whole surface. The drops may fall sporadically or all at once. In either case, they must strike the puddle surface at random points. The expanding circles of waves are the growth front of the spherulites, and the points of impact are the crystallite nuclei. Through probability derivations [27], the volume fraction of crystalline material, X, known widely as the degree of crystallinity, can be written as

$$1 - X = e^{-E} \quad (3)$$

where E is the average number of fronts of all such points in the system. For low degrees of crystallinity a useful approximation is $X \approx E$. For the bulk crystallisation of polymers, X in the exponent may be considered the volume or volume fraction of crystalline materials, V_t, i.e.

$$1 - X = e^{-V_t} \quad (4)$$

This has been the widely accepted and used equation in bulk crystallisation [28–40]. For either instantaneous or sporadic nucleation, Eq. (4) can be written as

$$1 - X = e^{-Kt^n} \quad (5)$$

where K is the growth rate, and n is the Avrami exponent, which depends not only on the structure of the crystal, but also on the nature of nucleation [41]. The Avrami exponent, n, is the phenomenological index of crystallisation, which can be used to discern between different mechanisms of crystallisation [32]. For example, when $n = 1$ it corresponds to rod-like growth from instantaneous nuclei; whereas $n = 3$ or 4 refers to spherulitic growth from either sporadic or instantaneous nucleation [42]. For polymer and organic systems, an n value of 2 or 3 indicates two- or three-dimensional nucleation of the crystal nucleus. However, fractional values of n also exist due to secondary crystallisation, e.g. lower n values (<1) are caused by linear crystal growth [37]. For ethylene/methacrylate blends, the Avrami exponent ranged from 2.75 to 6.42 [38].

The Avrami exponent is strongly affected by crystallisation temperature, in crystallisation of milk fat, the n values ranged from 0.5 to almost 5. At lower temperature (5 °C) the milk fat crystallised in the form of granules, whereas at higher temp (25 °C) they crystallised in the form of spherulites [32]. In the study on the kinetics of 5a-cholestan-3B-yl *N*-(2-naphthyl)carbamate/*n*-alkane organogel by Huang et al. [39], the gelation process involved one-dimensional growth and 'instantaneous nucleation' with the self-assembled fibrous network. However, the size and appearance changed abruptly from spherulitic to rod-like as the temperature of crystallisation was increased.

In this study, the degree of crystallinity is measured by the relative wax deposition, δ_r, defined as the mass fractions of the depositions on the wall and on the baffles of the OBTA divided

by the initial mass of the wax–oil liquid, i.e.

$$\delta_r = \frac{\delta_t - \delta_0}{\delta_\infty - \delta_0} \quad (6)$$

where δ_t is the total deposition at time t (min), δ_∞ the maximum or asymptotic deposition obtained from the deposition curves when the asymptotic condition or quasi-steady state has been achieved (g); δ_0 is the initial mass of the wax content in liquid (g). Replacing X by δ_r and taking log twice in Eq. (5) it becomes,

$$\log[-\ln(1 - \delta_r)] = \log K + n \log(t) \quad (7)$$

By plotting the left side in Eq. (7) versus $\log(t)$, the slope of the straight line n and the intersection K can be obtained. This information is used to evaluate the wax deposition process in the OBTA.

3. Materials and methods

The schematic diagram of the batch OBTA used in this study is shown in Fig. 1. The OBTA was made of a jacketed glass column of 25 mm in internal diameter, 50 mm in jacket diameter and 130 mm in height, giving a total liquid capacity of 64 ml and a working fluid capacity of 60 ml.

A K-type thermocouple is located within the OBTA and connected to a computer via Multipurpose Lab Interface (MPLI) supplied by Vernier Software Inc., USA, to record temperature profiles inside the column. A set of two stainless steel baffles of 3 mm thickness were used in this study and designed to fit closely to the wall of the column. The baffles are spaced 35 mm apart and supported by two 1.2 mm diameter stainless steel rods. The orifice diameter was 14 mm, creating a baffle free area of 30%. The baffle set was connected to the shaft of a piston through a supporting plate and driven by an electrical motor. Oscillation frequencies in the range of 0.1–5 Hz were controlled using a digital speed controller. Oscillation amplitudes of 2.5–15 mm (centre-to-peak) were generated by adjusting the preset distance between the linkage and the fly arm.

A peristaltic pump (Watson Marlow 505S) was used to circulate the heating and cooling water from two water baths. The maximum operating speed of the pump was 220 rpm. Both water baths are temperature-controlled, and cooling is achieved by circulating refrigerant (water + ethylene glycol) through a brass coil from a refrigerator (Julabo F200). Cooling rates were controlled by varying the flow rates of cooling water via the peristaltic pump speed (rpm).

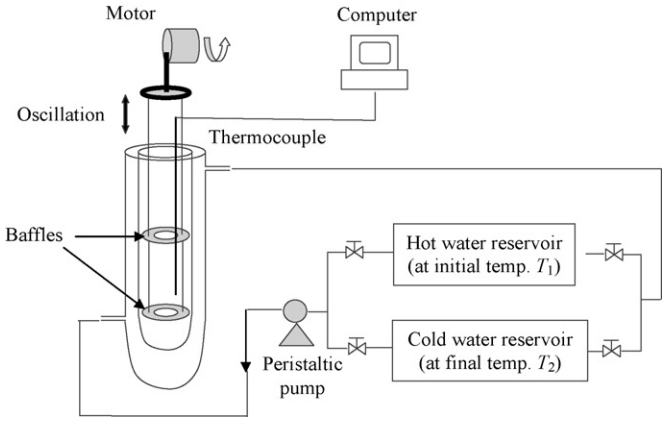

Fig. 1. Schematic diagram of oscillatory baffled tube apparatus (OBTA).

Paraffin wax was purchased from Aldrich Chemical, UK, and was in the form of solid chunks that was ground into powdery form. The melting point of the wax was reported in the range of 52–58 °C. Standard diesel was used as the model oil. The gravimetric method was employed to quantify the percentage of wax deposition.

The main focus of this investigation was on the effect of paraffin wax content of the wax–diesel solution used in the OBTA together with the effect of oscillation frequency (f) and amplitude (x_o). Four paraffin contents have been tested, i.e. 10, 20, 40 and 60% by weight representing four different supersaturation levels in terms of the crystallisation process. The values for the oscillation frequencies (f) examined were 1, 2 and 4 Hz, whereas for the amplitude (x_o) were 5, 10 and 15 mm, giving the oscillatory Reynolds numbers from 1359 to 8155 for 10% wax concentration; from 822 to 4934 for 20%; from 164 to 984 for 40% and from 37 to 224 for 60%. The initial hot temperature (T_1) was set at 50 °C which was well above the cloud point of the wax–oil solutions where no cloudiness observed for all solutions, and the final cold temperature (T_2) was selected at 10 °C. The speed of the cooling water pump (C_w) was set at 100 rpm ensuring a fixed cooling rate for all experiments. The cooling starts at $t = 0$ s.

The typical experimental duration is 10 min, and three wax deposit measurements were conducted at an interval of 1 min for the initial 3 min, followed by two measurements taken at an interval of 2 min for the middle 4 min, and finally one measurement taken at the end of the experiment time of 10 min. When carrying out measurements of wax deposit, the experiment was stopped, the column was dismantled from its supporting platform and the non-crystallised wax–oil was drained out of the column to a beaker and weighed. The crystallised wax inside the column was determined by the difference between the weight of the empty column and the weight of the column with the deposit. The deposit was then calculated as a percentage from the total wax–oil solution used. After the measurement, the experiment was restarted by recombining the solid deposit with the liquid part and the mixture was reheated to 50 °C.

It should be noted that the oil pipelines mentioned in the introduction are continuous operation, while our experiments are carried out in batch mode. This is because the fact that the fluid mechanical conditions in a batch OBTA are highly reproducible; and can easily and directly be applied to continuous processes. The eddy motions and intensity generated by oscillating baffles can be replicated by pulsing fluid. The results of our investigation in the batch set up will provide the much needed understanding of the principles in continuous operation. In addition, the batch OBTA can also be used as a simple test of the performance of wax inhibitors if we first understand the inhibited system. As to the question of how to apply oscillatory motion via oscillating baffles in existing pipelines, similar mixing conditions can be achieved using tubes/pipes with corrugated walls [46,47] at the

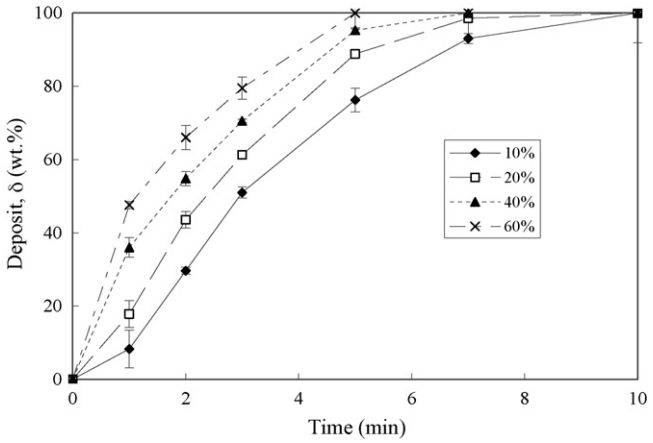

Fig. 2. Effect of paraffin wax content on the deposition in absence of oscillation.

appropriate flow rate of fluid. Hence, our studies in the batch device are highly relevant.

4. Results and discussion

In order to assess the effect of baffle oscillation on the wax deposition, control experiments were carried out in the OBTA with the presence of baffles, but without oscillation. Observations from the experiments were that the wax deposit was in the form of an oil gel, and the hardness of the gel increased with the content of the paraffin wax. The gel-like wax was adhered to the baffle surfaces and the wall of the column, while the liquid that flowed out from the centre of the column was a clear fluid. When 100% wax deposition has been reached, the gel-like wax filled the whole tube and became solidified. Fig. 2 shows the percentage of the wax deposition for different contents of paraffin wax in the control runs, where the *y*-axis corresponds to the percentage of wax deposited.

From the graph it can clearly be observed that the higher the paraffin content (the supersaturation level), the more wax deposit produced at any given time; the faster the deposition rates; and the quicker it reaches the 100% wax deposition. These results are well expected: with the increase of the paraffin wax content in solution, there are more wax molecules available to produce wax crystals.

Fig. 3 compares the percentage deposition from the control runs with those from the oscillation experiments for the wax content of 10, 20, 40 and 60% at a fixed oscillation

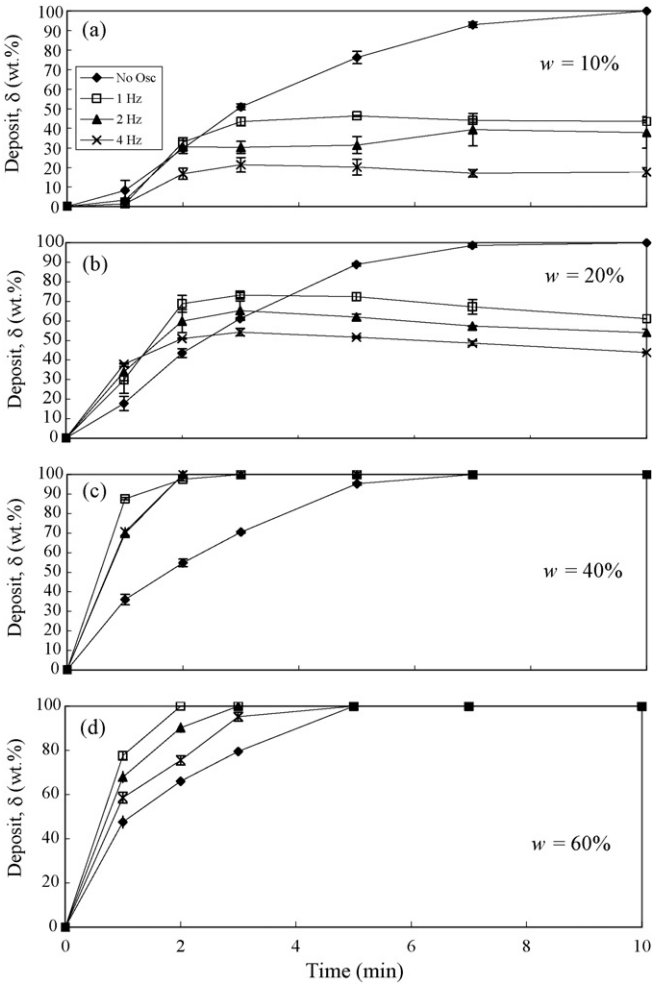

Fig. 3. Effect of oscillation frequencies on wax deposition for a range of paraffin content (x_o = 15 mm, St = 0.133, T_1 = 50 °C, T_2 = 10 °C).

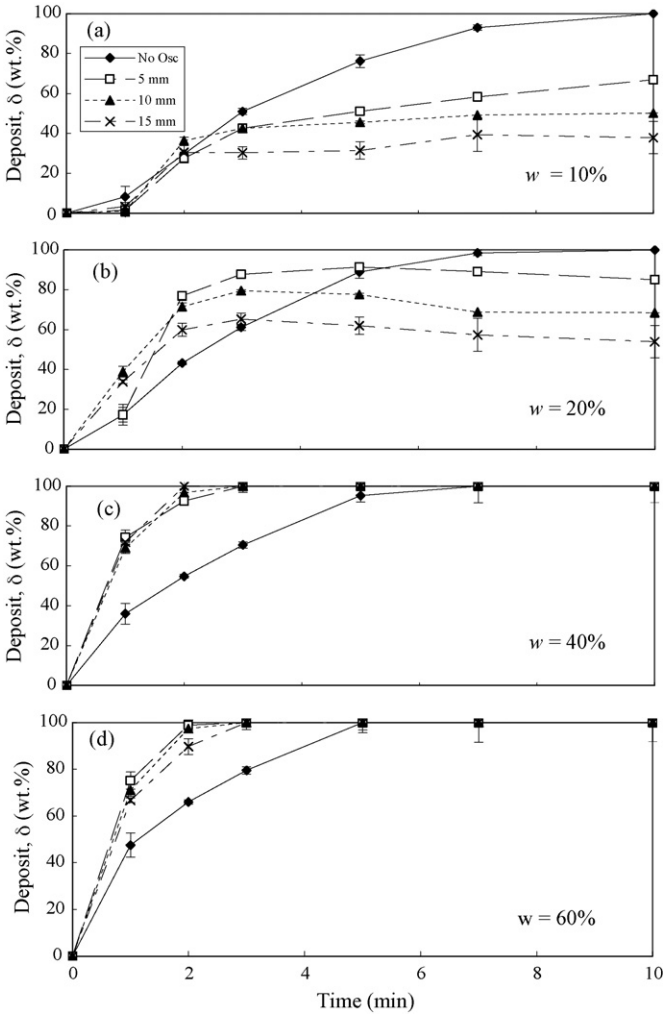

Fig. 4. Effect of oscillation amplitude on wax deposition for a range of paraffin content (f = 2 Hz, T_1 = 50 °C, T_2 = 10 °C).

amplitude or Strouhal number. In Fig. 3a with 10% paraffin wax content, the oscillatory motion reduced the deposition in comparison to the control results. At the end of experiments, the degree of the reduction is remarkable, e.g. about 60% reduction for 1 Hz; 70% for 2 Hz and over 80% for 4 Hz. Oscillatory motion effectively enables the wax crystals to remain suspended in the liquid, which minimises the contact time for crystals with the surface of the OBTA. In all cases 100% wax deposition has been avoided. The results clearly demonstrated that oscillatory motion has a beneficial effect in reducing wax deposition without the use of any solvent or wax inhibitor.

Fig. 3b shows the corresponding deposition curves for experiments with 20% paraffin wax content. The reduction of the wax deposition is still clearly seen, e.g. about 30% for 1 Hz, 40% for 2 Hz and 50% for 4 Hz, and once again 100% wax deposition has been prevented. However, the extent of reduction is less in comparison to Fig. 3a, reinforcing that the wax content of the solution or supersaturation level plays a major role in the deposition process. In fact, the oscillatory motion in this condition gave faster rates of the deposition in the first 2 min than in the control runs. The situation becomes more pronounced when the wax content is increased to 40% (Fig. 3c) and 60% (Fig. 3d), where the oscillation exhibits the opposite

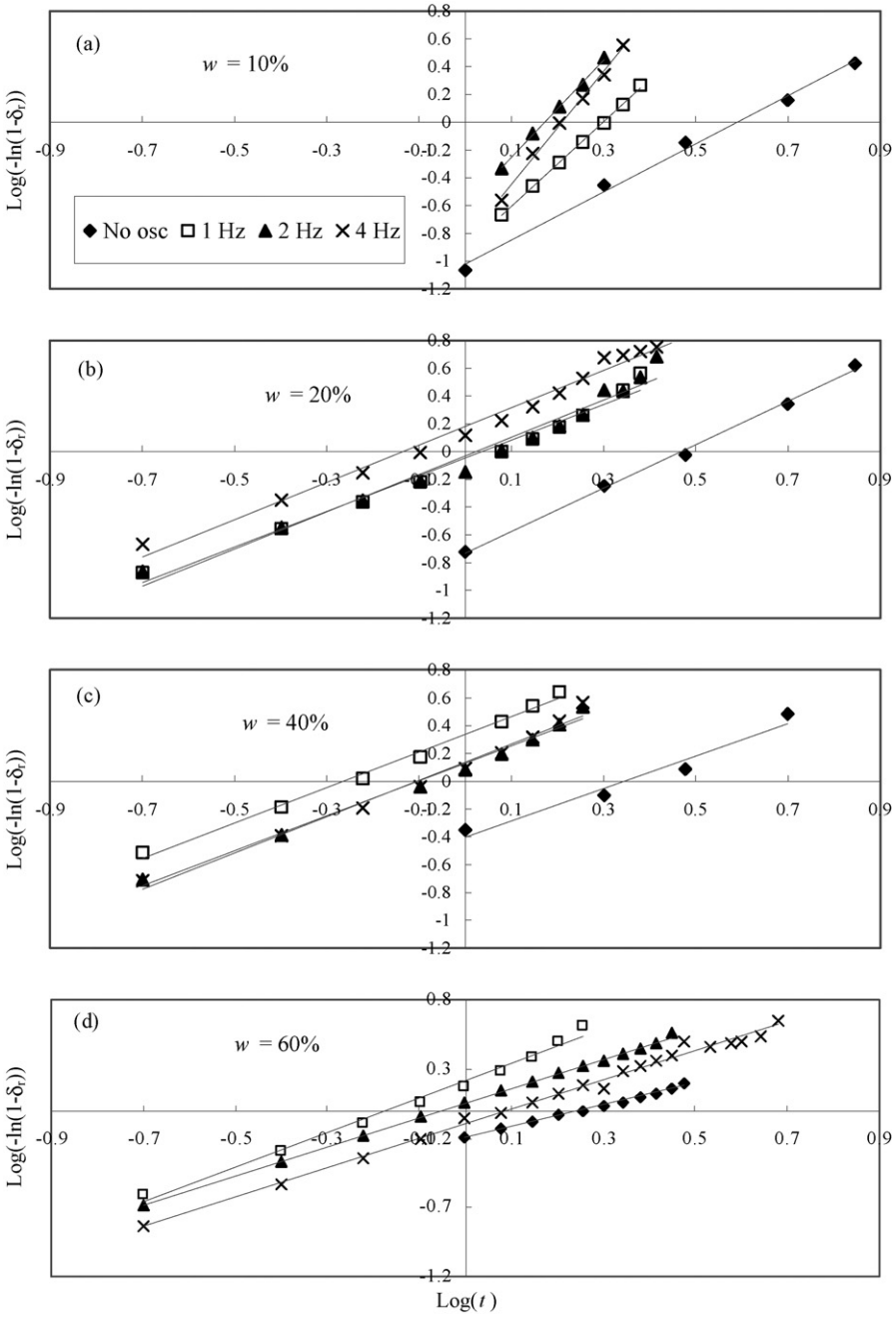

Fig. 5. The Avrami plots for different wax content showing the effects of oscillation frequencies (x_o = 15 mm, St = 0.133). The solid lines show the linear trend.

effect, i.e. enhancing the wax deposition on surfaces, not only with faster rates, but also with much shorter time for 100% deposition in comparison to the results of the control runs. The possible explanation would be that the enhancement of mixing encourages the cooling process of the solution in the OBTA, hence, allowing wax crystals in contact with internal surfaces more frequently at much shorter time and effectively promoting either instantaneous or sporadic nucleation. Note that the trend of the percentage wax deposition in Fig. 3d is that there is a faster wax deposition rate for 1 Hz than that for 4 Hz. This is likely due to the fact that reduced agitation led to longer contact time with the wall at such supersaturation level.

The effect of oscillation amplitude on percentage wax deposition as shown in Fig. 4 is similar to that in Fig. 3, but with lesser effective reduction of wax deposition. The results indicate that the oscillatory motion can have either beneficial or detrimental effect on the percentage deposition depending on the wax content in solution. For the wax content of 10–20%, the beneficial effect prevails. On the other hand, for the wax content greater than 20%, the detrimental effect dominates. In the real world, the wax content of crude oil is generally less than 20%, e.g. Leon-

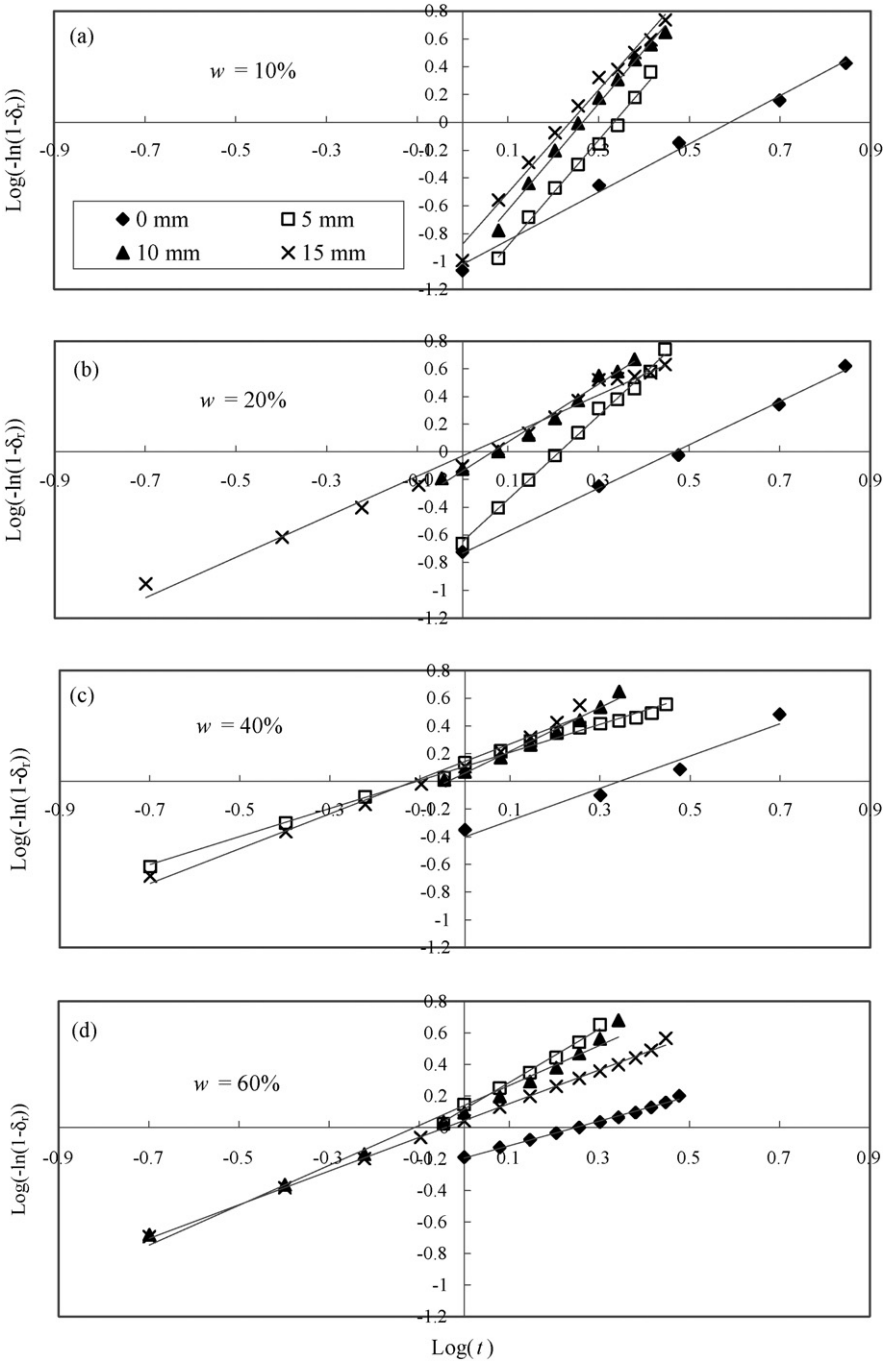

Fig. 6. Avrami plot for different wax content showing the effects of oscillation amplitudes (f = 2 Hz). The solid lines show the linear trend.

Table 1
Extracted Avrami parameters from Fig. 5 for the effect of oscillation frequency (x_o = 15 mm, St = 0.133)

Wax content (wt. %)	f = 0 Hz		f = 1 Hz		f = 2 Hz		f = 4 Hz	
	n	K (min^{-1})	n	K (min^{-1})	n	K (min^{-1})	n	K (min^{-1})
10	*1.73*	0.10	*3.05*	0.12	*3.70*	0.13	*4.08*	0.14
20	1.56	0.19	1.28	0.90	1.46	0.93	1.34	1.51
40	1.17	0.40	1.27	2.18	1.26	1.39	1.31	1.37
60	0.78	0.64	1.26	1.64	1.07	1.11	1.06	0.80

Table 2
Extracted Avrami parameters from Fig. 6 for the effect of oscillation amplitude (f = 2 Hz)

Wax content (wt. %)	x_o = 0 mm		x_o = 5 mm (St = 0.398)		x_o = 10 mm (St = 0.199)		x_o = 15 mm (St = 0.133)	
	n	K (min^{-1})	n	K (min^{-1})	n	K (min^{-1})	n	K (min^{-1})
10	*1.73*	0.10	*3.80*	0.05	*3.83*	0.10	*3.70*	0.13
20	1.56	0.19	3.03	0.23	2.08	0.73	1.46	0.93
40	1.17	0.40	1.01	1.28	1.58	1.14	1.26	1.39
60	0.78	0.64	1.70	1.30	1.27	1.38	1.07	1.11

taritis and Mansoori [43] reported that the Venezuelan Boscan crude contained around 17% waxy materials.

5. Kinetic analysis

From the wax deposition profiles presented earlier, wax formation can generally be divided into two main sections: the growth phase and the quasi-steady (or the asymptotic) state. Typically the growth phase took place in the first 2 min of the experiments for all the wax solutions. By analysing the growth phase curves using the Avrami theory, some crystallisation/deposition kinetics can be extracted. Figs. 5 and 6 plot $\log[-\ln(1-\delta_r)]$ versus $\log(t)$ for the effect of oscillation frequency and amplitude, respectively. From these figures, good linearity can be seen for both cases, indicating the effectiveness of the Avrami methodology. The Avrami exponent (n) and the rate constant (K) are extracted from the plots (as explained in Section 2) and summarised in Tables 1 and 2.

In both tables, some general trends can be observed. First, the growth rate (K) generally increases with the wax content in solution or supersaturation level with some exceptions. This is expected, as the higher wax concentration or supersaturation, the more wax crystals, the higher crystallisation rate. Secondly, the Avrami exponent decreases with the increase of the wax concentration in solution. This suggests different growth forms of crystals for different wax concentrations. Thirdly, for higher wax concentrations or supersaturations, both n and K are largely similar for different frequencies and amplitudes, suggesting that the effect of oscillation on the crystallisation mechanism is insignificant under these conditions. As the 10% wax concentration in solution is closely associated with the real crude oil systems, both n and K values are further analysed.

The most noticeable increase in n in Tables 1 and 2 can be seen for the 10% wax concentration, where a step change is clearly visible between the cases with and without oscillation. Using both n and K as the diagnostic tool of crystallisation mechanism, Hay [26] derived a model for spheres, discs and rods, representing three-, two- and one-dimensional forms of growth, which are summarised in Table 3. It suggests that although the growth rates (K) are similar, the wax crystals produced in the presence of oscillation tend to be spherical, in comparison to rod-like shape in the absence of oscillation. The results may underline the transition mechanism for the beneficial effect of oscillatory motion on the reduction of wax deposition. Without the oscillation, the wax crystals would be of rod-like shape in one dimensional growth; these rods would spread to the walls and baffle surfaces, resulting in gel-formation and crystals precipitated out of solution. When the oscillatory motion is applied at 10% wax concentration, the Avrami constants approach four suggesting sporadic nucleation, and the net result of the motion is to change the rod-like crystals into sphere-like crystals. With the help of a microscope and a scanning electron microscope, Fig. 7 shows the microscopic shapes of the crystals obtained with and without oscillation. Clearly the shapes of the crystals shown in Fig. 7 are matched well with the kinetic evaluations. It seems that the sphere-like crystals are less likely to be gelled on the internal surfaces of the OBTA; however, it is not fully understood as to why the changes in the crystallisation mechanism would cause the reduction of wax deposition.

Table 3
The Avrami parameters for crystallisation of polymers [26]

Crystallisation mechanism	n	Growth form
Spheres		
Sporadic	4	Three dimensions
Instantaneous	3	Three dimensions
Discs[a]		
Sporadic	3	Two dimensions
Instantaneous	2	Two dimensions
Rods[b]		
Sporadic	2	One dimension
Instantaneous	1	One dimension

[a] Constant thickness.
[b] Constant radius.

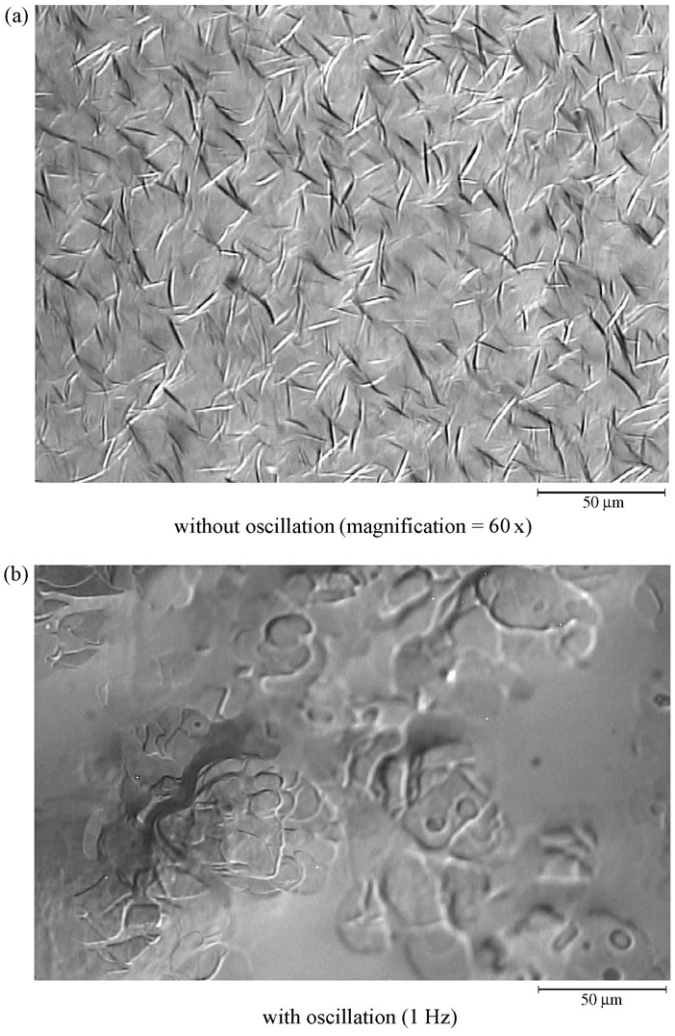

Fig. 7. Microscopic images of samples taken from solution containing 10% wax (magnification = 60×).

6. Conclusion

The study shows that the oscillatory motion has two opposite effects on wax deposition within the OBTA: at low wax concentration, the oscillatory motion significantly reduced the percentage of wax deposition, e.g. 40–60% without the use of any solvent or wax inhibitor; and completely prevented 100% wax deposition from happening – the beneficial effect; at higher wax contents, on the other hand, the introduction of oscillatory motion not only promoted wax deposition, but also speeded up the rates to achieve 100% gelation. From the Avrami analysis, it is found that the increase of the wax content in solution generally reduces the Avrami exponent, while increases the growth rate, suggesting that the crystallisation growth form is shifted from multi- to one-dimensional, with instantaneous nucleation predominating.

The most interesting results obtained at 10% wax concentration are that the Avrami exponent experienced a step change increase in the presence of oscillation in comparison to these without. This suggests the oscillatory motion has altered the growth form—the most important factor on the percentage of wax deposition; resulting the significant reduction in the wax deposition in OBTA.

Acknowledgements

LI wishes to acknowledge Universiti Teknologi PETRONAS, Tronoh, Malaysia, for sponsoring his PhD programme and Heriot-Watt University, Edinburgh, Scotland for the placement and research facilities.

References

[1] F.S. Ribeiro, P.R.S. Mendes, S.L. Braga, Obstruction of pipelines due to paraffin deposition during the flow of crude oils, Int. J. Heat Transf. 40 (18) (1997) 4319–4328.
[2] J.L. Creek, H.J. Lund, J.P. Brill, M. Volk, Wax deposition in single phase flow, Fluid Phase Equilibr. 158–160 (1999) 801–811.
[3] V.A.M. Branco, G. Mansoori, L.C.D.A. Xavier, S.J. Park, H. Manafi, Asphaltene flocculation and collapse from petroleum fluids, J. Petrol. Sci. Eng. 32 (2001) 217–230.
[4] S.M. Al-Zahrani, T.F. Al-Fariss, A general model for the viscosity of waxy oils, Chem. Eng. Process. 37 (1998) 433–437.
[5] H. Li, J. Zhang, A generalized model for predicting non-Newtonian viscosity of waxy crudes as a function of temperature and precipitated wax, Fuel 82 (2003) 1387–1397.
[6] J.Y. Zuo, D.D. Zhang, H.J. Ng, An improved thermodynamic model for wax precipitation from petroleum fluids, Chem. Eng. Sci. 56 (2001) 6941–6947.
[7] H. Manafi, G.A. Mansoori, S. Ghotbi, Phase behaviour prediction of petroleum fluids with minimum characterisation data, J. Petrol. Sci. Eng. 22 (1999) 67–93.
[8] J.A.P. Coutinho, R. Szczepanski, X. Zhang, Reliable wax predictions for flow assurance, in: Presented at the SPE 13th European Petroleum Conference Paper SPE 78324, Aberdeen, Scotland, UK, October 29–31, 2002.
[9] P. Singh, A. Youyen, H.S. Fogler, Existence of critical carbon number in the aging of a wax–oil gel, AIChE J. 47 (9) (2001) 2111–2124.
[10] J.S.T. dos Santos, A.C. Fernandes, M. Giulietti, Study of the paraffin deposit formation using the cold finger methodology for brazilian crude oils, J. Petrol. Sci. Eng. 45 (2004) 47–60.
[11] P. Singh, R. Venkatesan, H.S. Fogler, Formation and aging of incipient thin film wax–oil gels, AIChE J. 46 (5) (2000) 1059–1074.
[12] A. Matzain, M.S. Apte, H.Q. Zhang, M. Volk, J.P. Brill, J.L. Creek, Investigation of paraffin deposition during multiphase flow in pipelines and wellbores. Part 1: Experiments, J. Energ. Resour. Technol. 124 (2002) 180–186.
[13] M. Li, J. Su, Z. Wu, Y. Yang, S. Ji, Study of the mechanisms of wax prevention in a pipeline with glass inner layer, Colloid. Surf. A 123 (124) (1997) 635–649.
[14] T.R. Bott, J.S. Gudmundsson, Deposition of paraffin wax from kerosene in cooled heat exchanger tubes, Can. J. Chem. Eng. 55 (1977) 381–385.
[15] A.J. Cordoba, C.A. Schall, Application of heat transfer method to determine wax deposition in a hydrocarbon binary mixture, Fuel 80 (2001) 1285–1291.
[16] A.J. Cordoba, C.A. Shall, Solvent migration in a paraffin deposit, Fuel 80 (2001) 1279–1284.
[17] I.M. El-Gamal, Combined effects of shear and flow improvers: the optimum solution for handling waxy crudes below pour point, Colloid. Surf. A 135 (1998) 283–291.
[18] R.C. Sarmento, G.A.S. Ribbe, L.F.A. Azevedo, Wax blockage removal by inductive heating of subsea pipleines, Heat Transf. Eng. 25 (7) (2004) 2–12.
[19] E. Marie, Y. Chevalier, S. Brunel, F. Eydoux, L. Germanaud, P. Flores, Settling of paraffin crystals in cooled middle distillates fuels, J. Colloid Interface Sci. 269 (2004) 117–125.
[20] B.F. Towler, S. Rebbapragada, Mitigation of paraffin wax deposition in cretaceous crude oils of wyoming, J. Petrol. Sci. Eng. 45 (2004) 11–19.
[21] N.P. Tung, N.Q. Vinh, N.T.P. Phong, B.Q.K. Long, P.V. Hung, Perspective for using Nd–Fe–B magnets as a tool for the improvement of the produc-

tion and transportation of vietnamese crude oil with high paraffin content, Physica B 327 (2002) 443–447.
[22] P. Singh, H.S. Fogler, Fused chemical reactions: the use of dispersion to delay reaction time in tubular reactors, Ind. Eng. Chem. Res. 37 (1998) 2203–2207.
[23] M. Avrami, Kinetics of phase change I. general theory, J. Chem. Phys. 7 (1939) 1103–1112.
[24] U.R. Evans, The laws of expanding circles and spheres in relation to lateral growth of surface films and the grain size of metals, T. Faraday Soc. 41 (1945) 365–374.
[25] P. Meares, Polymers: structure and bulk properties, Van Norstrand, London, 1965.
[26] J.N. Hay, Application of the modified Avrami equations to polymer crystallisation kinetics, Br. Polym. J. 3 (2) (1971) 74–82.
[27] L.H. Sperling, Kinetics of crystallisations, in: L.H. Sperling (Ed.), Introduction to Physical Polymer Science, John Wiley and Sons, New York, 1986, pp. 177–191.
[28] C. Caze, E. Devaux, A. Crespy, J.P. Cavrot, A new method to determine the Avrami exponent by D.S.C. studies of non-isothermal crystallisation from the molten state, Polymer 38 (3) (1997) 497–502.
[29] M.T. Connor, M.C.G. Gutierrez, D.R. Rueda, F.J.B. Calleja, Cold crystallisation studies on PET/PEN blends as revealed by microhardness, J. Mater. Sci. 32 (1997) 5615–5620.
[30] M.G. Lu, M.J. Shim, S.W. Kim, Curing behaviour of unsaturated polyester system analysed by Avrami equation, Thermochim. Acta 323 (1998) 37–42.
[31] A.R. Bhattacharyya, T.V. Sreekumar, T. Liu, S. Kumar, L.M. Ericson, R.H. Hauge, R.E. Smalley, Crystallisation and orientation studies in polypropylene/single wall carbon nanotube composite, Polymer 44 (2003) 2373–2377.
[32] R.J. Campos, J.W. Litwinenko, A.G. Marangoni, Fractionation of milk fat by short-path distillation, J. Dairy Sci. 86 (2003) 735–745.
[33] D.Z. Chen, P.S. He, L.J. Pan, Cure kinetics of epoxy-based nanocomposites analysed by Avrami theory of phase change, Polym. Test. 22 (2003) 689–697.
[34] H. Luo, J. Sietsma, S. van der Zwaag, Effect of inhomogeneous deformation on the re-crystallisation kinetics of deformed metals, ISIJ Int. 44 (11) (2004) 1931–1936.
[35] J.W. Litwinenko, A.P. Singh, A.J. Marangoni, Effects of glycerol and Tween 60 on the crystallisation behaviour, mechanical properties, and microstructure of plastic fat, Cryst. Growth Des. 4 (1) (2004) 161–168.
[36] W. Li, X. Kong, E. Zhou, D. Ma, Isothermal crystallisation kinetics of poly(ethylene terephthalate)–poly(ethylene oxide) segmented copolymer with two crystallising blocks, Polymer 46 (2005) 11655–11663.
[37] S. Pal, A.K. Nandi, Cocrystallisation mechanism of poly(3-alkyl thiophenes) with different alkyl chain length, Polymer 46 (2005) 8321–8330.
[38] R.P. Pereira, A.M. Rocco, Nanostructure and crystallisation kinetics of poly(ethylene oxide)/poly(4-vinylphenol-co-2-hydroxyethyl methacrylate) blends, Polymer 46 (2005) 12493–12502.
[39] X. Huang, P. Terech, S.R. Raghavan, R.G. Weiss, Kinetics of 5a-cholestan-3β-yl *N*-(2-naphthyl)carbamate/*n*-alkane organogel formation and its influence on the fibrillar networks, J. Am. Chem. Soc. 127 (12) (2005) 4336–4344.
[40] X. Wang, J.J. Vlassak, Crystallization kinetics of amorphous NiTi shape memory alloy thin films, Scripta Mater. 54 (5) (2006) 925–930.
[41] M. Avrami, Kinetics of phase change. II. Transformation–time relations for random distribution of nuclei, J. Chem. Phys. 8 (1940) 212–224.
[42] A. Sharples, Overall kinetics of crystallisation, in: A. Sharples (Ed.), Introduction to Polymer Crystallisation, Edward Arnold Ltd., London, 1966, pp. 44–59.
[43] K.J. Leontaritis, G.A. Mansoori, Asphaltene deposition: a survey of field experiences and research approaches, J. Petrol. Sci. Eng. 1 (1988) 229–239.
[44] H.-Y. Ji, B. Tohidi, A. Danesh, A.C. Todd, Wax phase equilibria: developing a thermodynamic model using a systematic approach, Fluid Phase Equilibria 216 (2) (2004) 201–217.
[45] N.P. Tung, N.Q. Vinh, N.T.P. Phong, B.Q.K. Long, P.V. Hung, Perspective for using Nd–Fe–B magnets as a tool for the improvement of the production and transportation of Vietnamese crude oil with high paraffin content, Physica B. 327 (2003) 443–447.
[46] T. Nishimura, Y. Kajimoto, A. Tarumoto, Y. Kawamura, Flow structure and mass transfer for a wavy channel in transitional flow regime, J. Chem. Eng. Japan 19 (1986) 449–455.
[47] T. Nishimura, S. Arakawa, S. Murakami, Y. Kawamura, Oscillatory viscous flow in symmetric wavy-walled channels, Chem. Eng. Sci. 44 (1989) 2137–2148.